GREAT DESIGNS IN STEEL

Mechanical Properties of Resistance Spot Welds: In-situ PWHT & Load–based Fracture Model Assessment

Olakunle Betiku

Mohammad Shojaee

Center for Advanced Materials Joining

Dept. of Mechanical & Mechatronics Engineering

University of Waterloo

Presentation Overview

GDIS

Part 1

Resistance spot welding

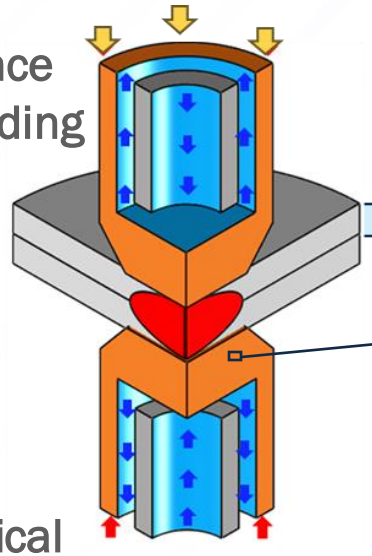

High cooling rate

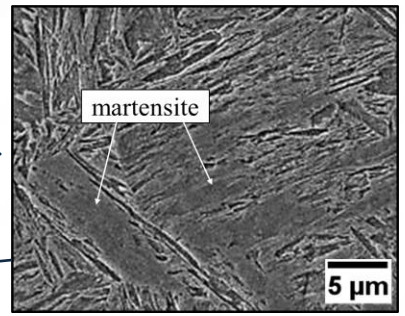

Martensite

Mechanical properties

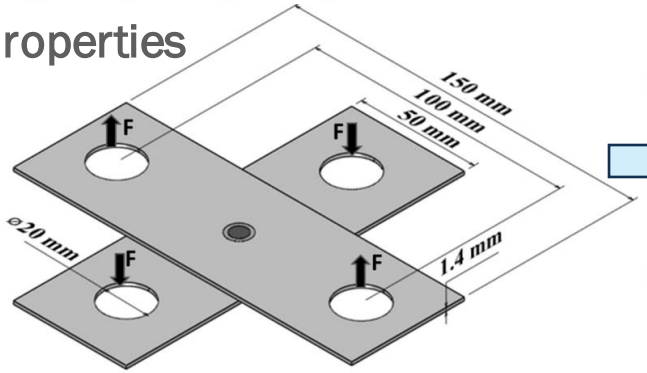

Relatively low energy absorption capability

What techniques can be used to modify the microstructure and improve the mechanical properties??

Part 2

Assessment of Conventional Three-dimensional Failure Surface for 3G-AHSS Resistance Spot Welds

$$f = \left[\frac{F_s}{S_S}\right]^a + \left[\frac{F_n}{S_N}\right]^b + \left[\frac{M_b}{S_B}\right]^c \leq 1$$

Shear Strength | Tensile Strength | Bending Strength

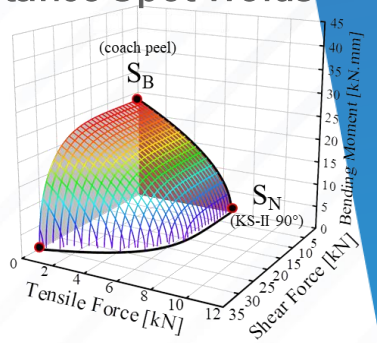

Shear/tensile loading (KS-II):

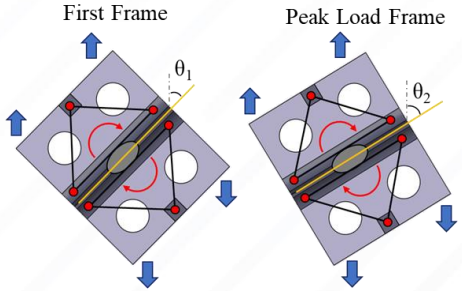

In plane rotation = $\Delta\theta = \theta_2 - \theta_1$

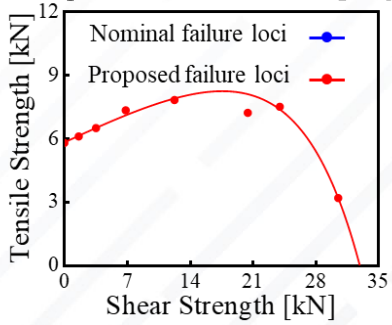

Tensile/bending loading (coach peel):

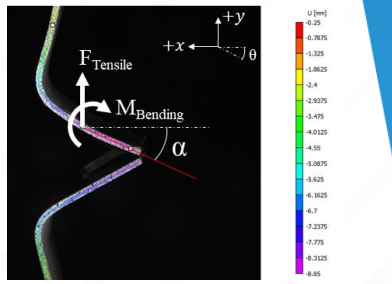

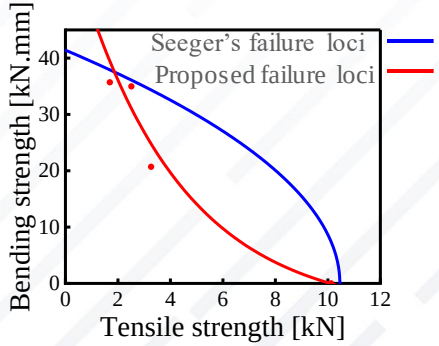

Motivation

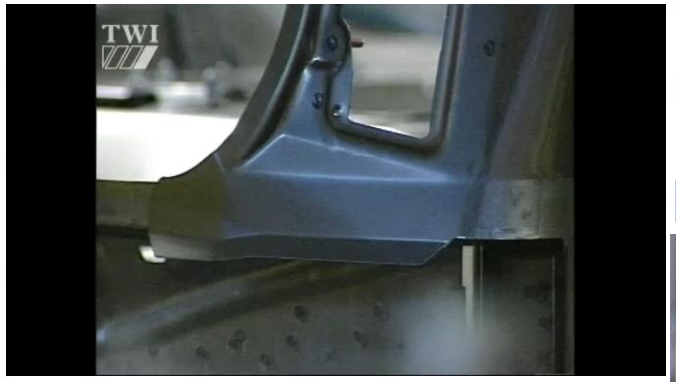

In simple terms, two sheet metals are joined

Processing

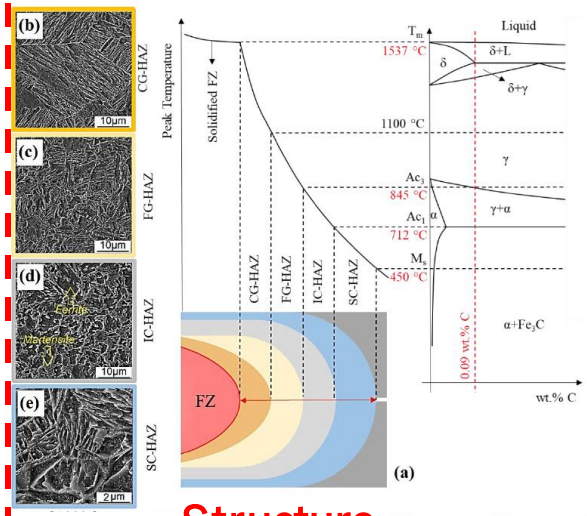

Structure

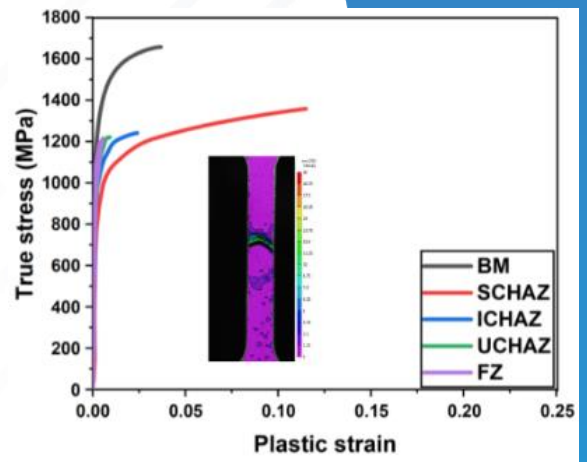

Properties

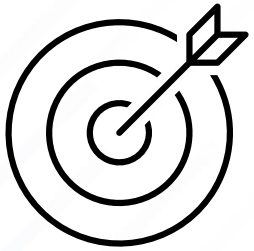

Apply an in-situ post weld heat treatment to improve joint properties

Midawi et al., Forces in Mechanics, 2022.

In-situ Post-weld Heat Treatment (PWHT)

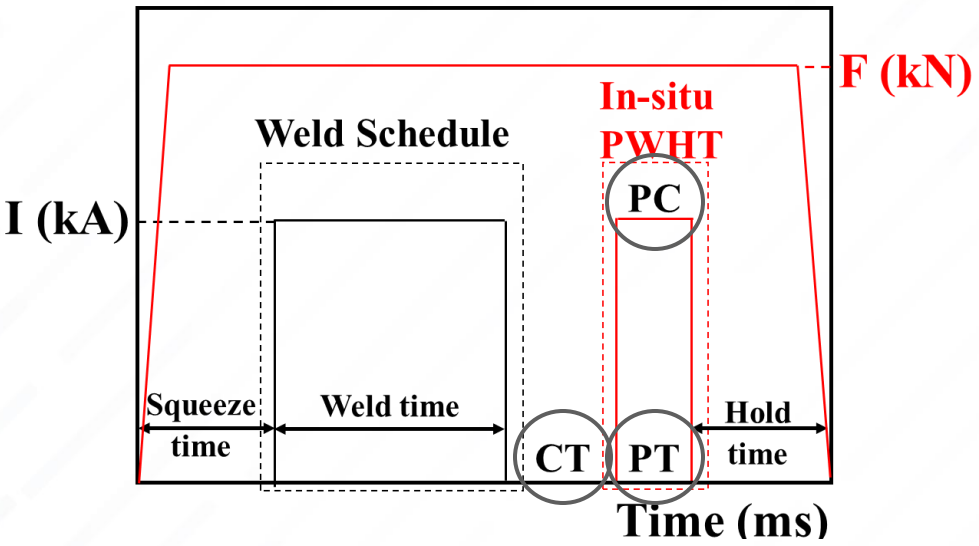

In-situ PWHT Parameters

- *CT: Cool time* Control
- *PT: Pulse time*
- *PC: Pulse current*

Metallurgical techniques
- ✓ Tempering
- ✓ Recrystallization

NEW

- Martensite **tempering** of the FZ (Betiku et al., 2022)
  - General consensus on **cool time**
  - **post weld current and time** depends on material chemical composition and/or thickness.
- **Recrystallization** (in-situ grain refinement) (Betiku et al., 2023)
  - Austenite recrystallization induces in-situ grain refinement.

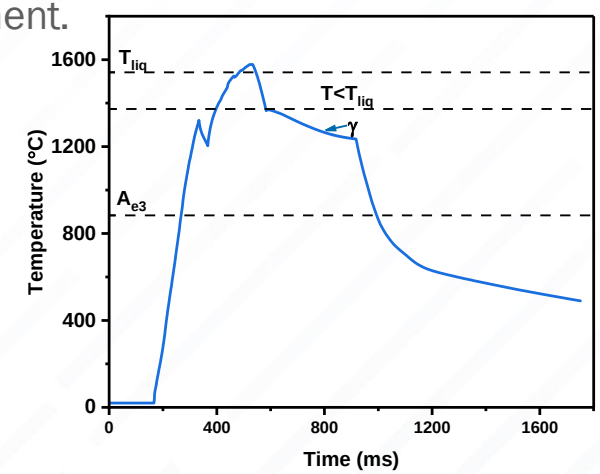

- **Slow cooling**: delay martensitic transformation.
- **Dual force technique**: induce strain-hardening
  - **How do these techniques compare in improving mechanical properties?**

Hernandez et al., Welding journal, 2012
Khan et al., SEA technical paper series, 2007
Eftekharimilani et al, STWJ, 2017

Material & Method

Material: Press-Hardened Steel

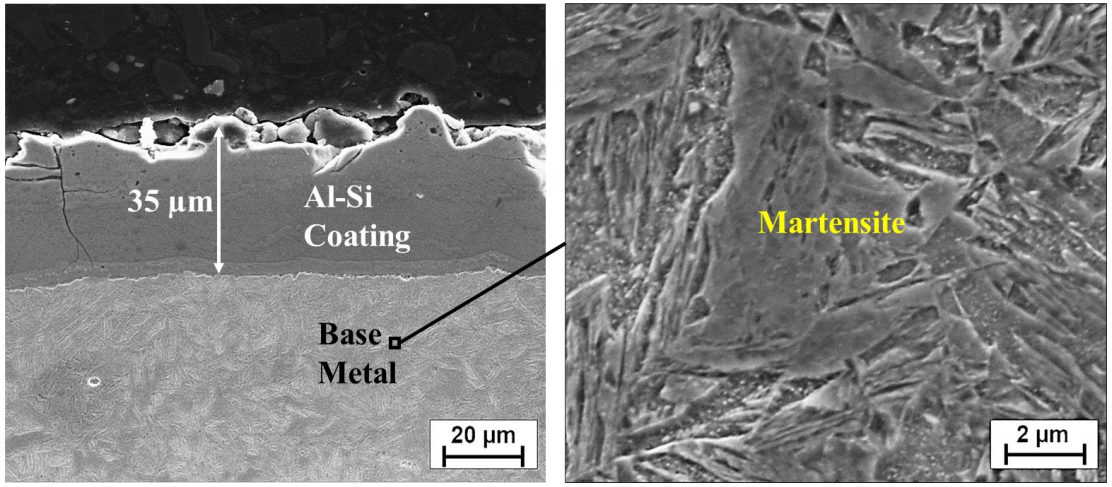

Microstructure after hot stamping

Material	Sheet thickness (mm)	Carbon equivalent	YS (MPa)	UTS (MPa)	T.E (%)	U.E (%)	Base metal hardness (HV)
PHS	1.4	0.47	1228±14	1623±13	6.89±0.50	4.66 ± 0.15	491 ± 4

RSW Baseline Schedule

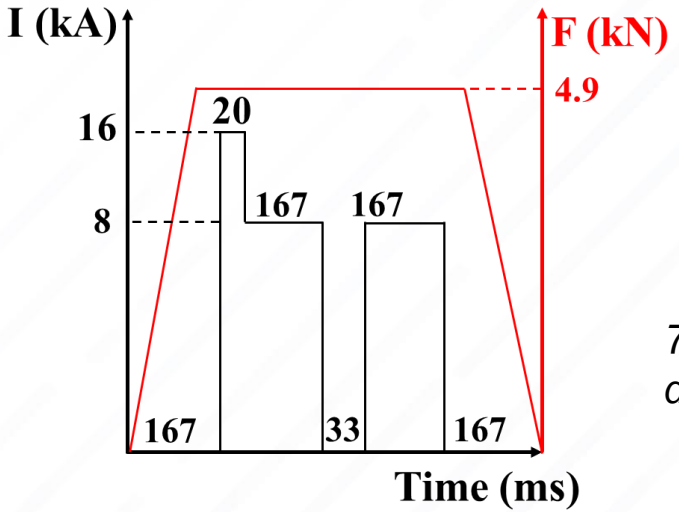

7 mm electrode diameter

Honda RSW Robot

Method

In-situ PWHT

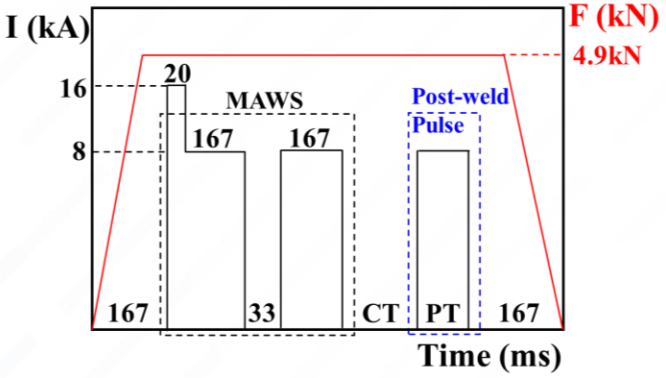

Weld schedule

Weld Schedule	Squeeze time (ms)	Weld Pulse 1 (ms)	Cool time (ms)	Weld Pulse 2 (ms)	Cool time 2 (ms)	Post-Pulse time (ms)	Hold time (ms)	Weld and post pulse (kA)
As-welded	167	167	33	167	-	-	-	8
Tempering	167	167	33	167	1000	67	167	8
ReCrX	167	167	33	167	100	167	167	8
Slow cool	167	167	33	167	100	900	167	6
Dual force	167	167	33	167	50	334	167	-

Slow cooling

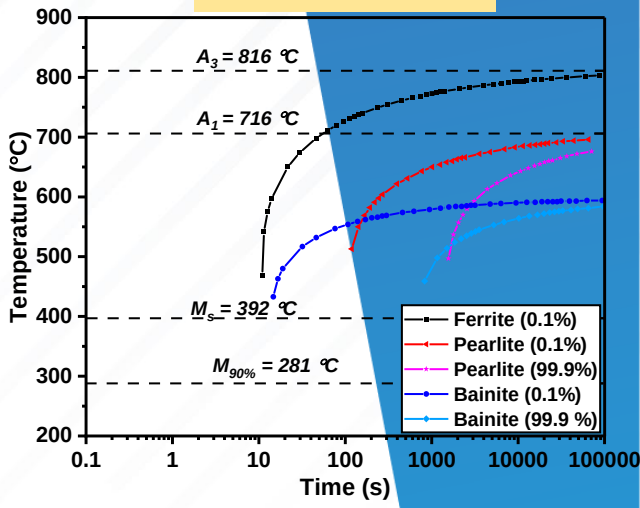

Dual force

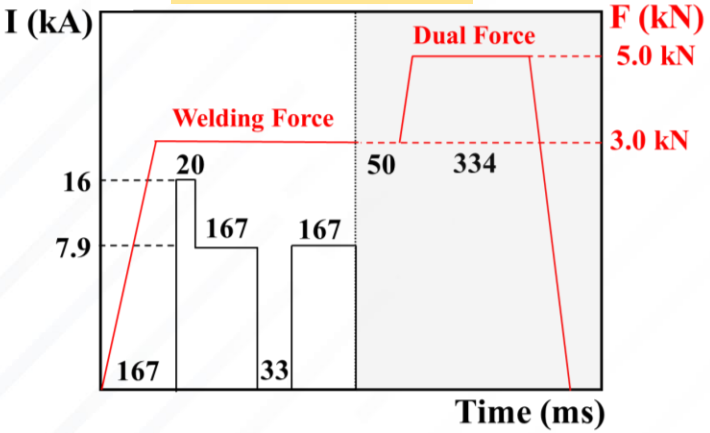

Mechanical properties (CTT)

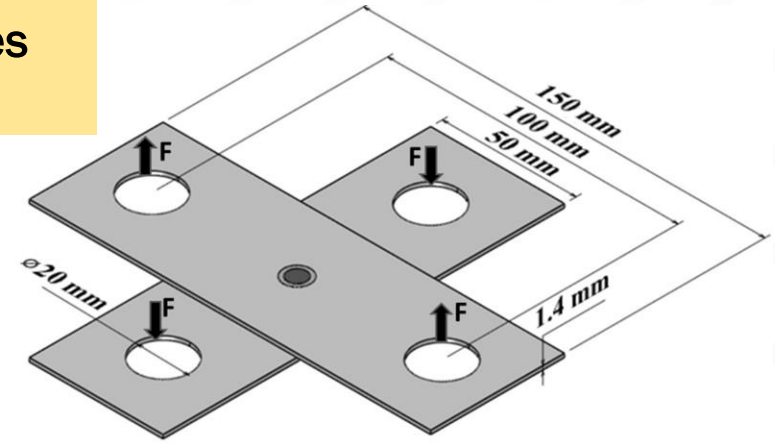

Microstructure

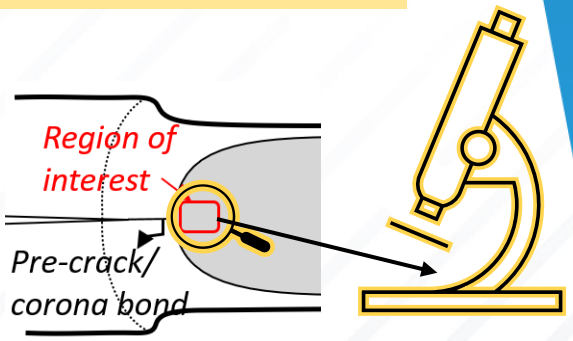

Results: Mechanical Properties

- ✓American welding schedule (AWS)
- ✓Tempering pulse
- ✓Recrystallization pulse (RecrX)
- ✓Slow cooling (S.Cool)
- ✓Dual Force (DF)

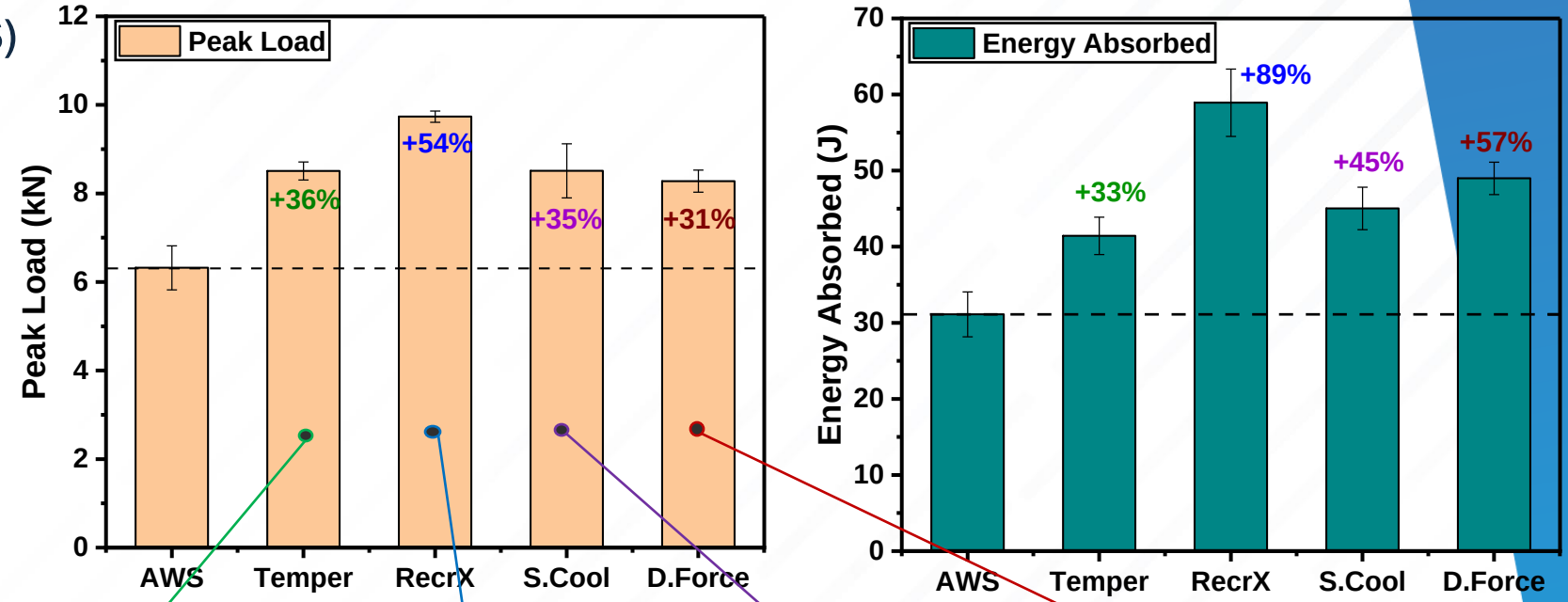

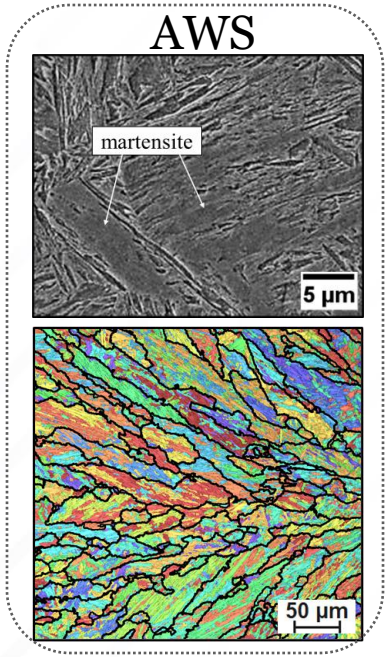

SEM

EBSD

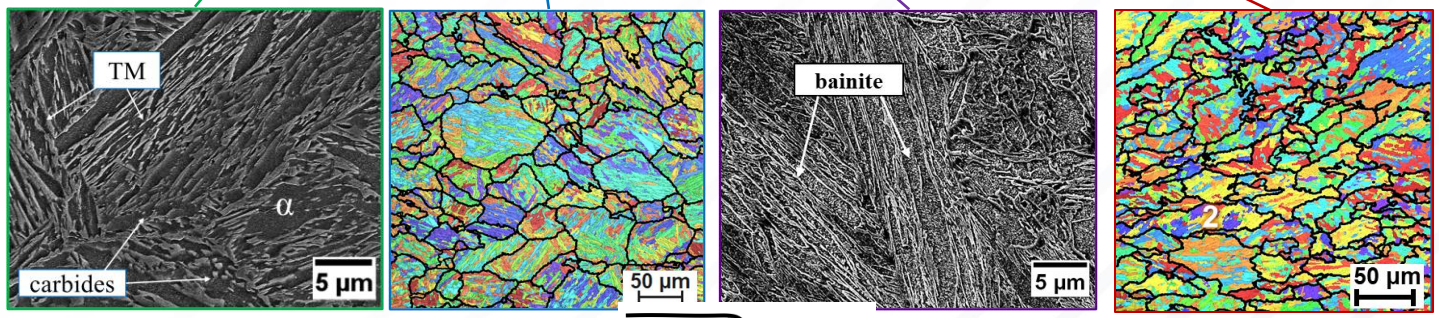

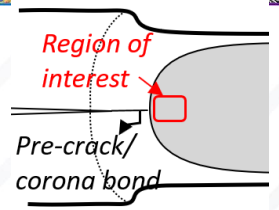

O.T Betiku et al, welding in the world, 2022.

Metallurgical Transformations

Mechanical Properties

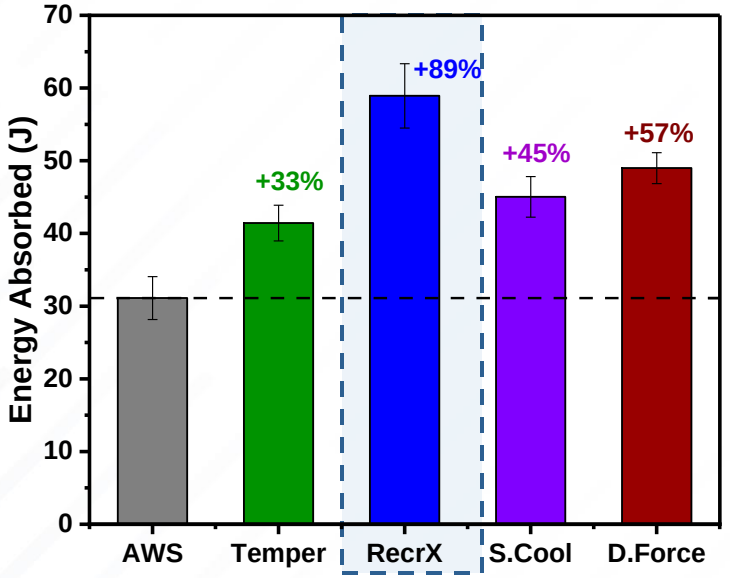

- ✓American welding schedule (AWS)
- ✓Tempering pulse
- ✓Recrystallization pulse (RecrX)
- ✓Slow cooling (S.Cool)
- ✓Dual Force (DF)

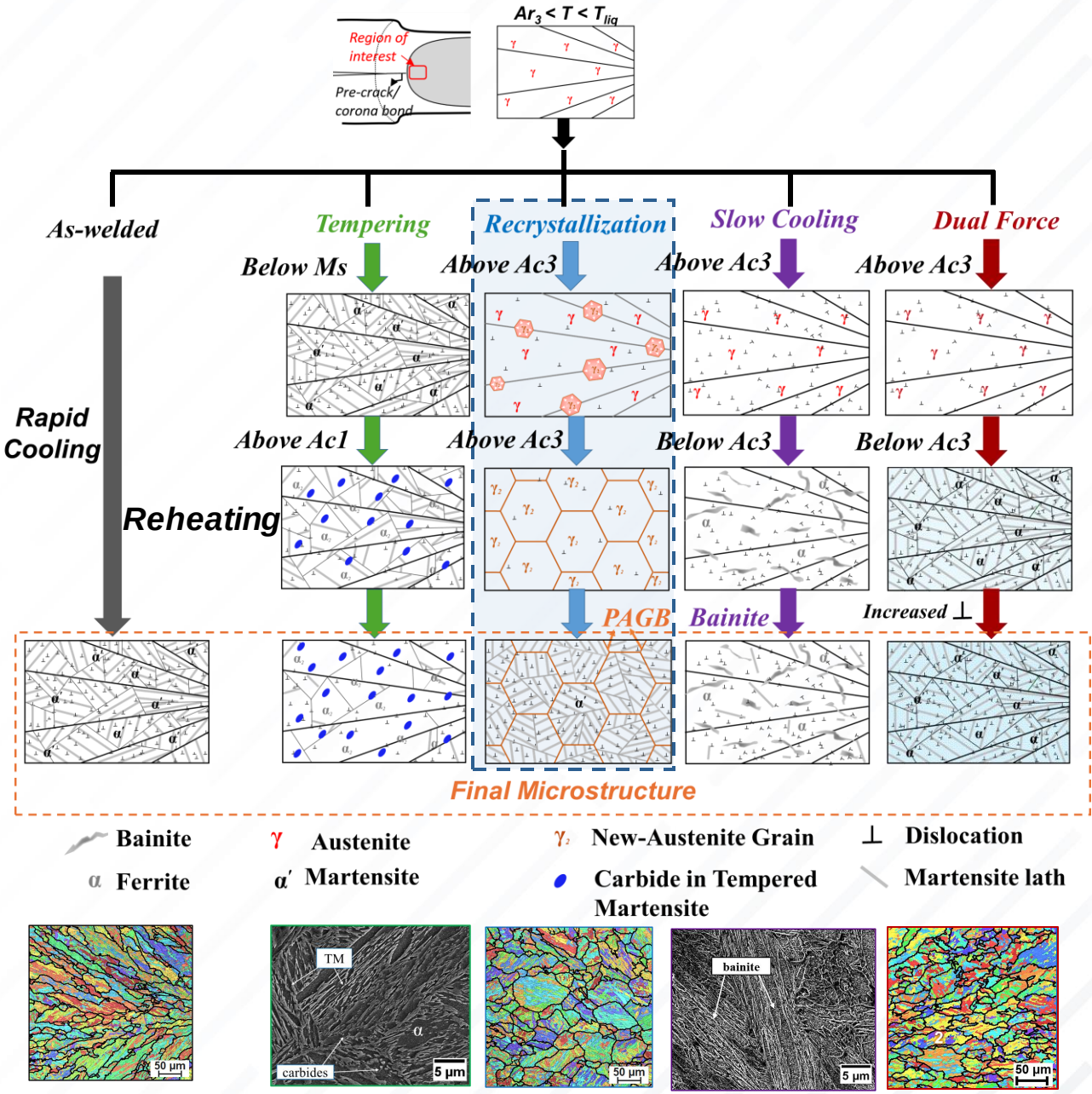

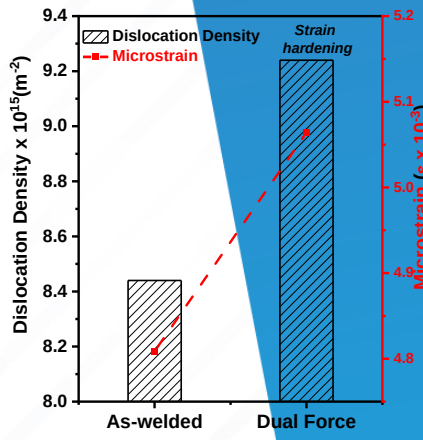

O.T Betiku et al, welding in the world, 2022.

Mechanical Properties & Process Time Comparison

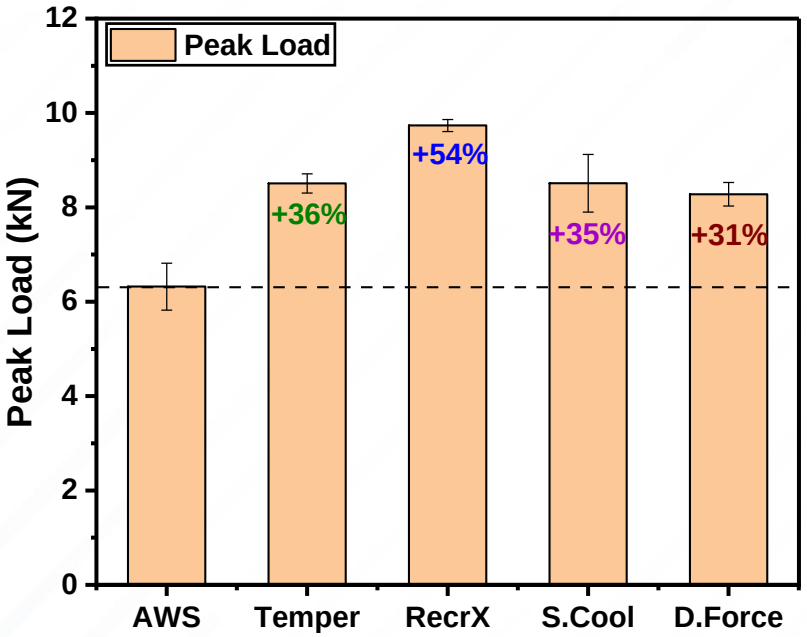

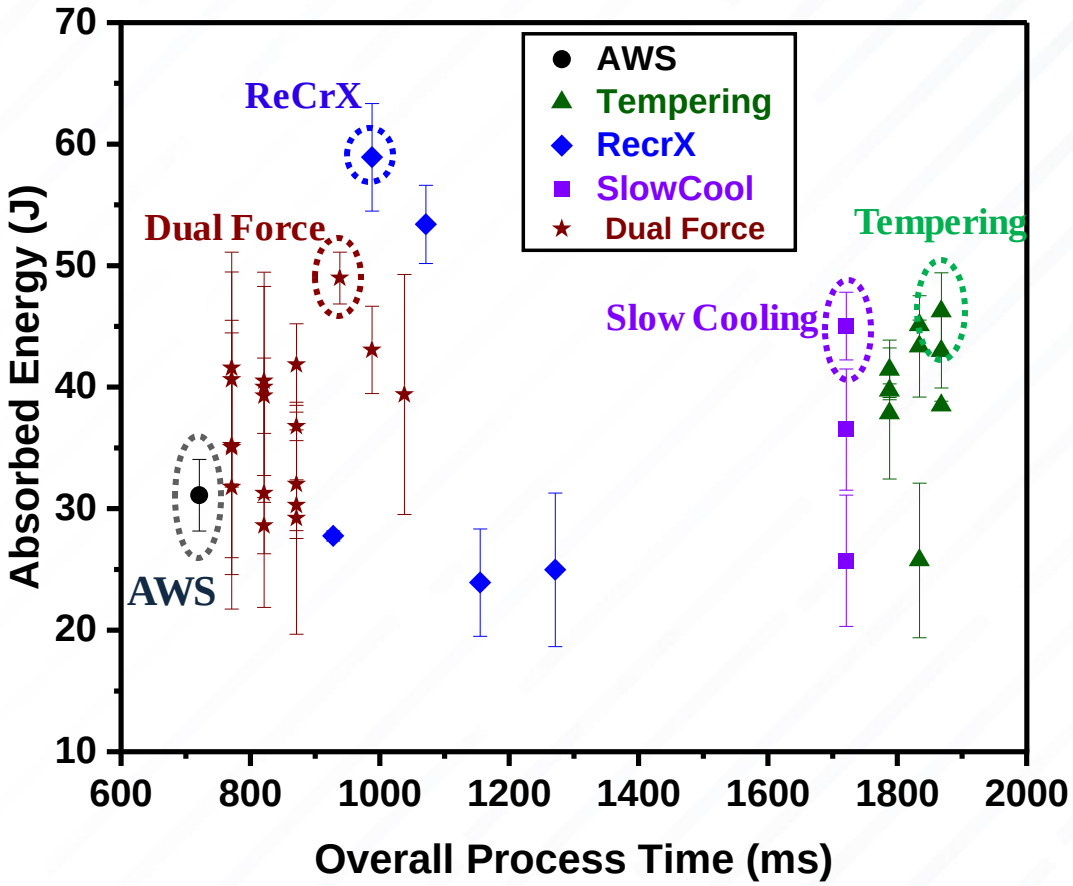

- In-situ grain refinement achieved via austenite recrystallization improves energy absorption capability by 89% with a reduced process time compared to tempering and slow cooling PWHT techniques.

Prediction of RSW Failure

2 approaches for RSW failure prediction:

1. Mesoscale models (fine mesh+ detailed fracture characterization of FZ, HAZ, and BM)

Informative regarding mechanics of fracture

Fine mesh- Computationally expensive

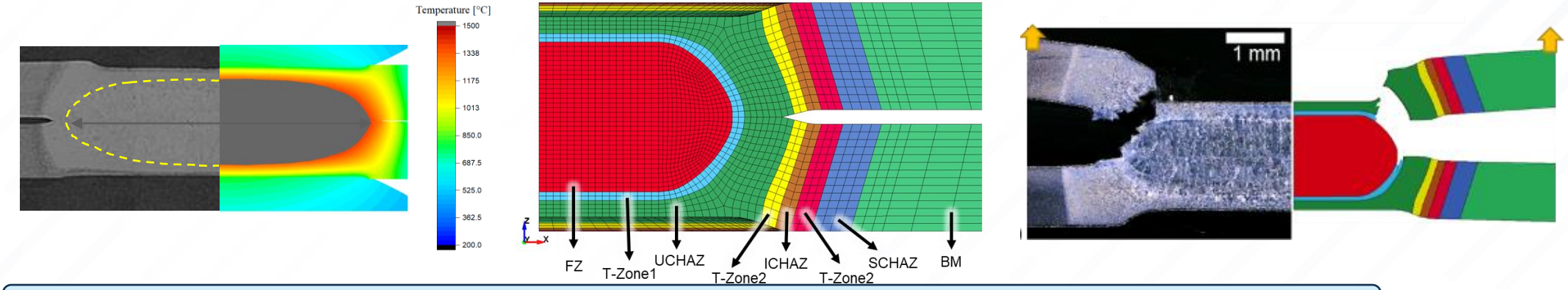

Development of fracture loci for various RSW sub-zone requires extensive experimentation.

2. CAE models (coarse mesh+ interpolated failure loci from mechanical tests)

Coarse mesh- Well-suited for industrial applications

Limited insight on mechanics of failure

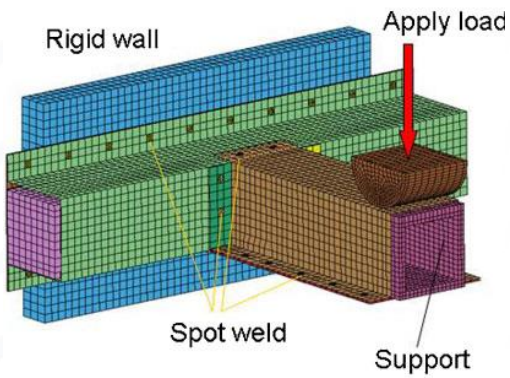

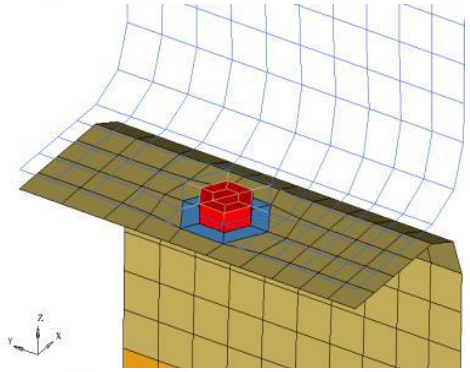

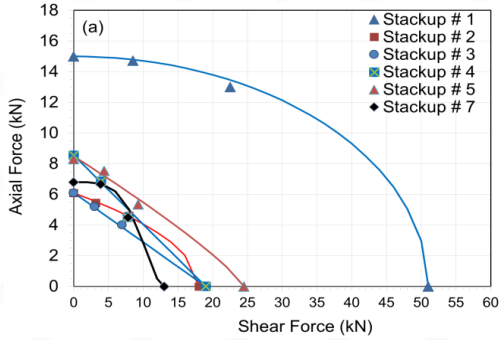

Alternatively, experimental failure loci can be calibrated in various loading conditions and used in force-based failure criteria to predict RSW failure.

[1] Mohamadizadeh Ph.D. Thesis (2020)
[2] Ghassemi-Armaki et al. *Int J Mech Sci* (2011)

Investigated Materials

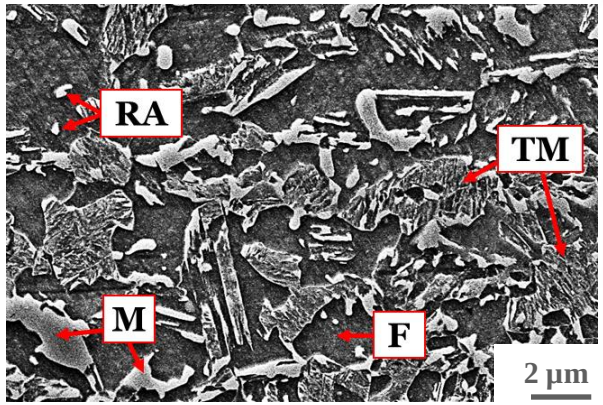

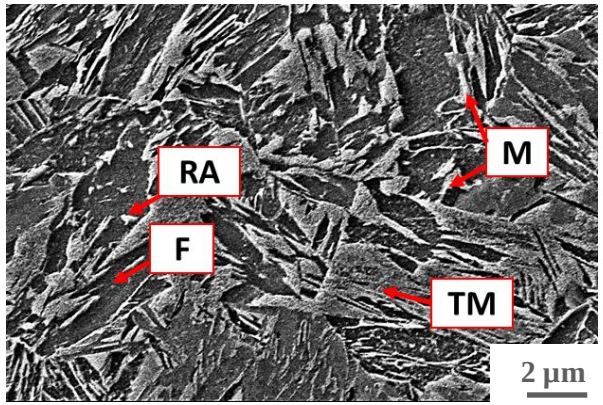

3G-980
Base material hardness:
300 ± 6 HV

3G-1180
Base material hardness:
380 ± 5 HV

Material	C	Mn	Si	Cr+Mo+V	Cu+Ni	C_{eq}
3G-980	0.21	2.11	1.49	0.02	<0.01	0.64
3G-1180	0.17	2.52	1.59	0.28	<0.02	0.70

Material	Sheet Thickness [mm]	YS [MPa]	UTS [MPa]	TE [%]	UE [%]
3G-980	1.4	605 ± 7.78	1002 ± 8.29	19.89 ± 0.50	16.8 ± 0.55
3G-1180	1.4	967 ± 7.05	1181 ± 19.02	11.83 ± 0.6	8.1 ± 0.35

YS, yield strength; UTS, ultimate tensile strength; TE, total elongation; UE, uniform elongation; 0.2% offset method was used to calculate YS

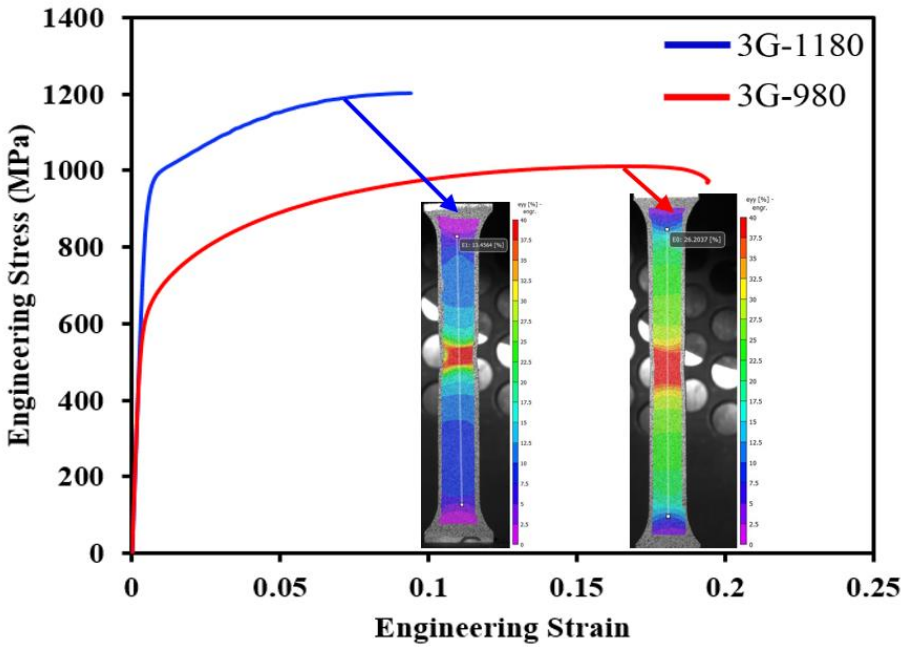

(a) 3G-980 FDWS of 7.0 mm

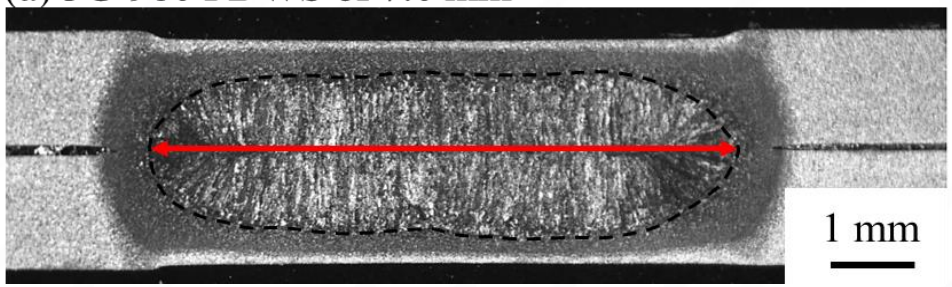

(b) 3G-1180 FDWS of 7.1 mm

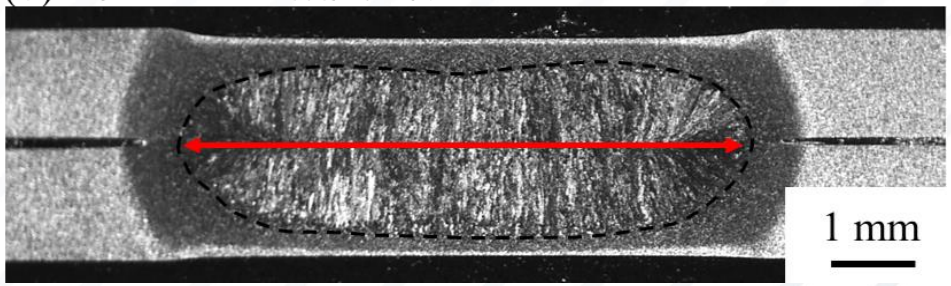

Objective

Seeger's suggested failure equation is incorporated in LS-DYNA MAT100 (2005):

$$f_{3D} = \left(\frac{\sigma_N(\dot{\varepsilon})}{S_N(\dot{\varepsilon})}\right)^{n_S} + \left(\frac{\sigma_B(\dot{\varepsilon})}{S_B(\dot{\varepsilon})}\right)^{n_B} + \left(\frac{\tau(\dot{\varepsilon})}{S_S(\dot{\varepsilon})}\right)^{n_N} < 1$$

Tensile strength — Bending strength — Shear strength

Constant strain rate

$$f^S = \left[\frac{F_s}{S_S}\right]^a + \left[\frac{F_n}{S_N}\right]^b + \left[\frac{M_b}{S_B}\right]^c \leq 1$$

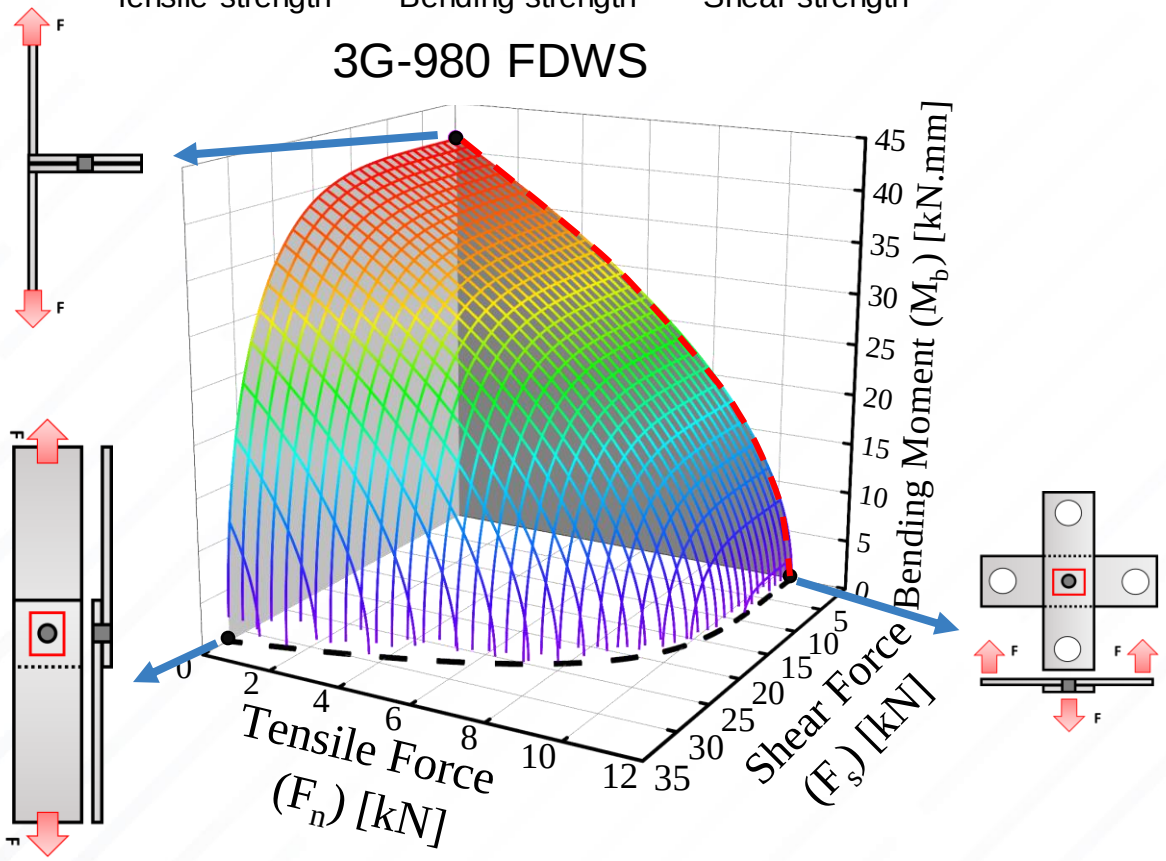

3G-980 FDWS

3G-1180 FDWS

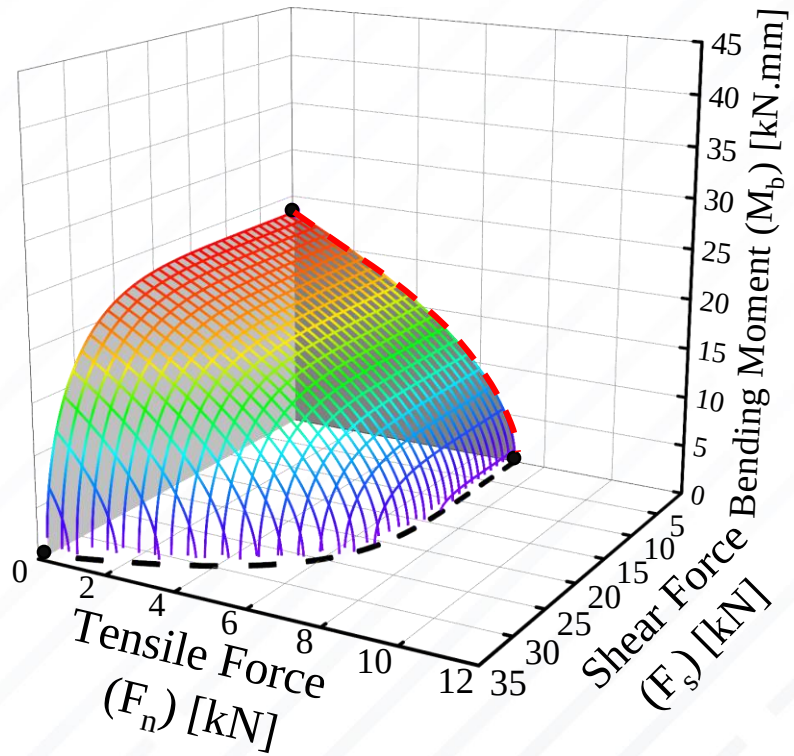

Assess validity of Seeger's 3D failure surface in two loading conditions:

1. Tensile-bending loading mode (red dashed lines in figures above)
2. Shear-tensile loading mode (black dashed lines in figures above)

Assessment of Seeger's Loci in Shear-Tensile Loading Conditions:

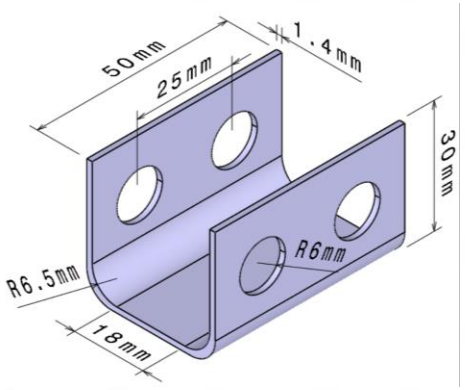

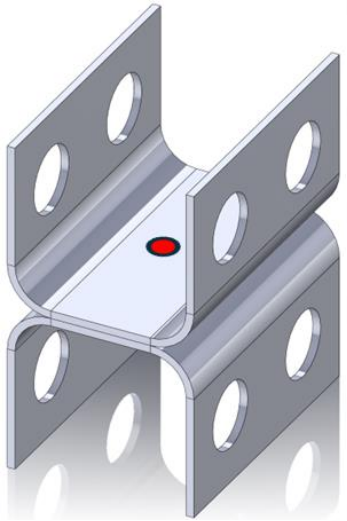

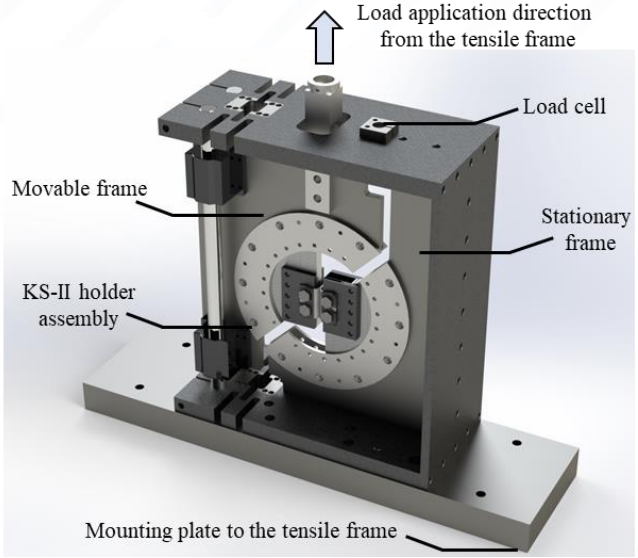

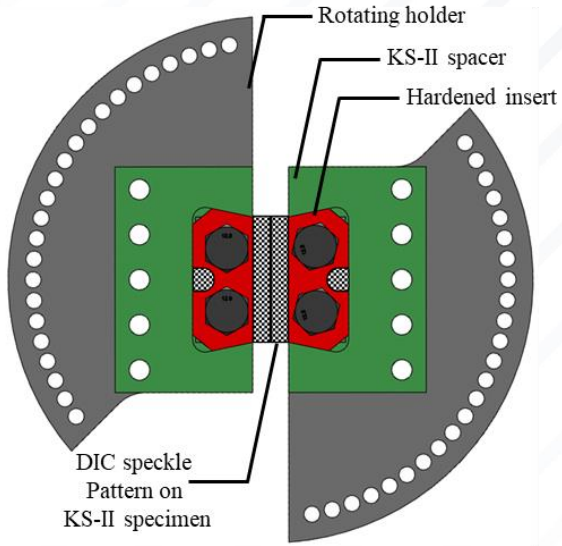

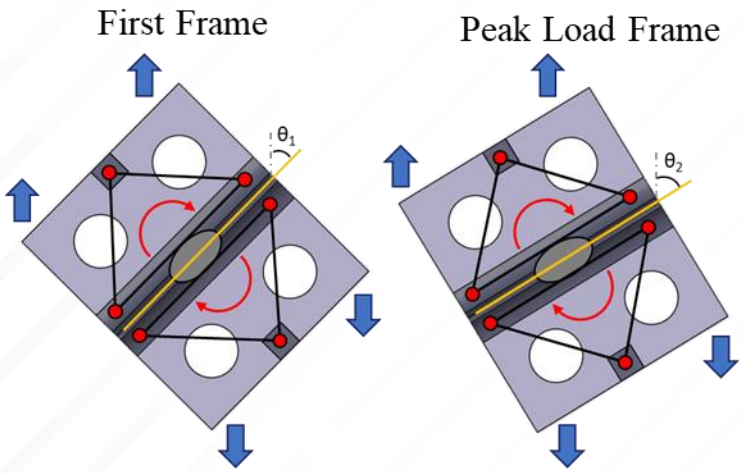

In plane rotation = $\Delta\theta = \theta_2 - \theta_1$

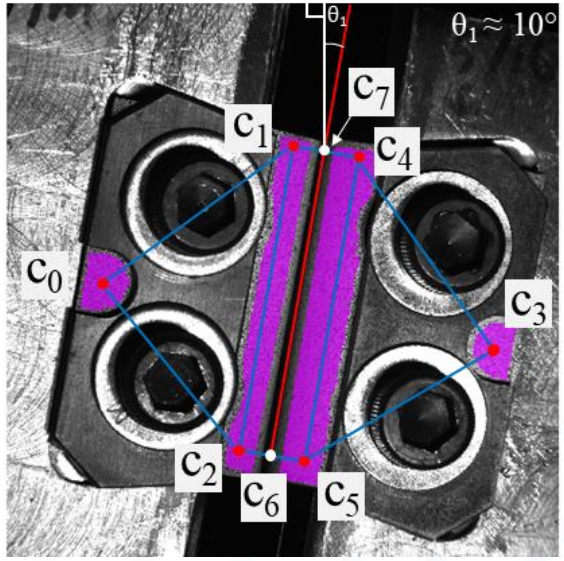

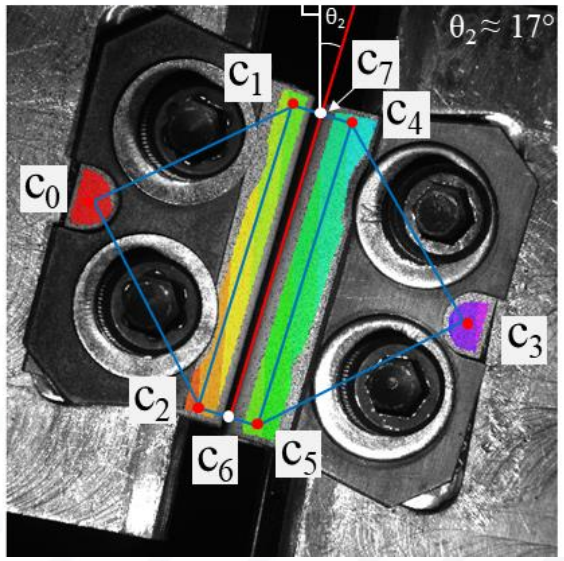

Assessment of Seeger's Loci in Shear-Tensile Loading Conditions:

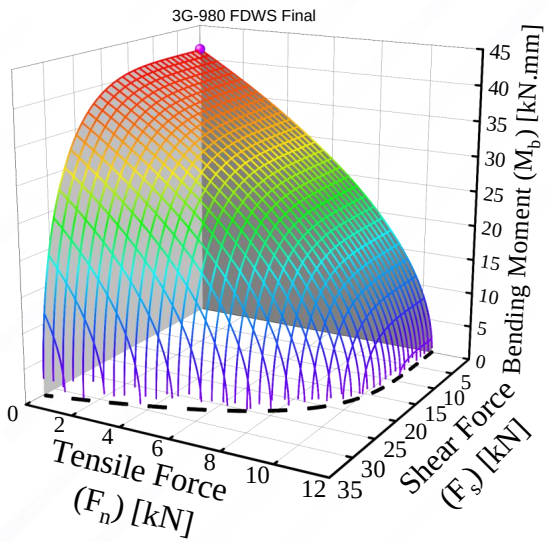

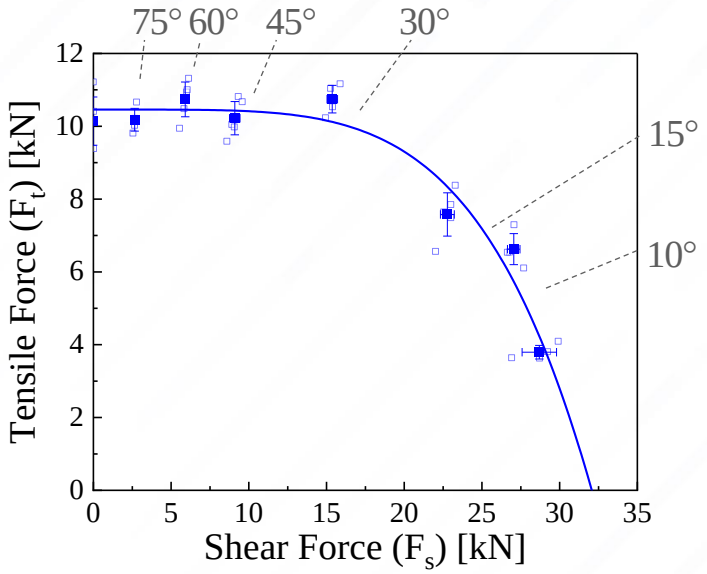

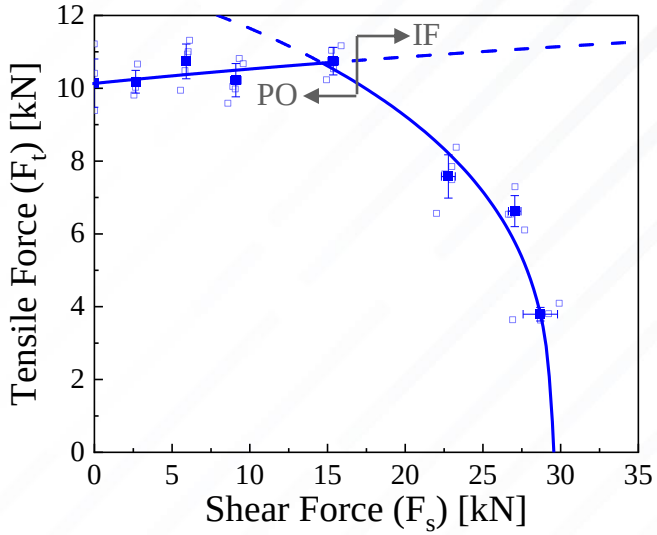

3G-980

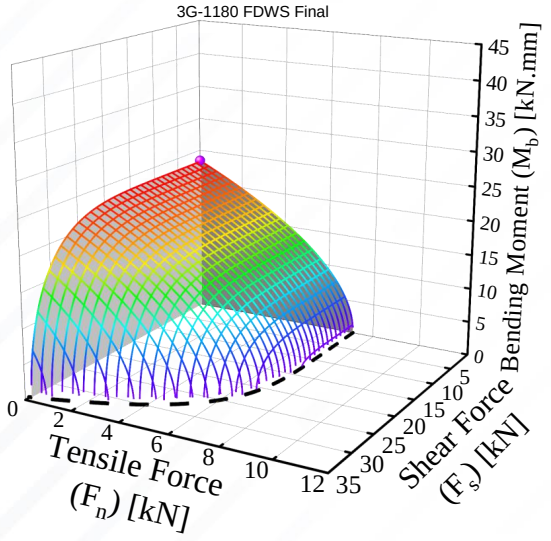

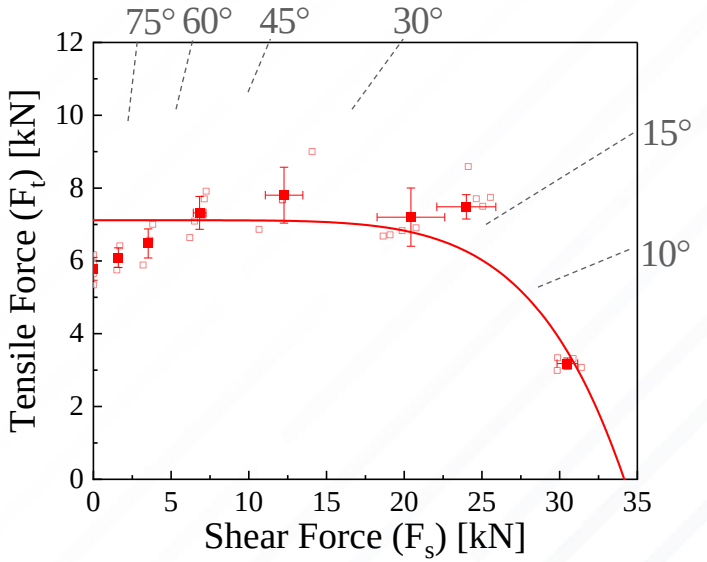

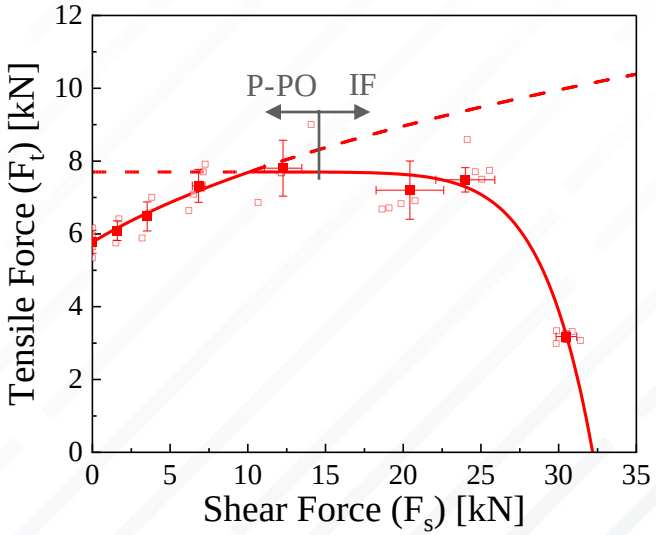

3G-1180

Average over-prediction of between 0.2% to 3.5% for shear-tensile loading based on Seeger's proposed failure loci

Assessment of Seeger's Loci in Tensile-bending Loading Conditions:

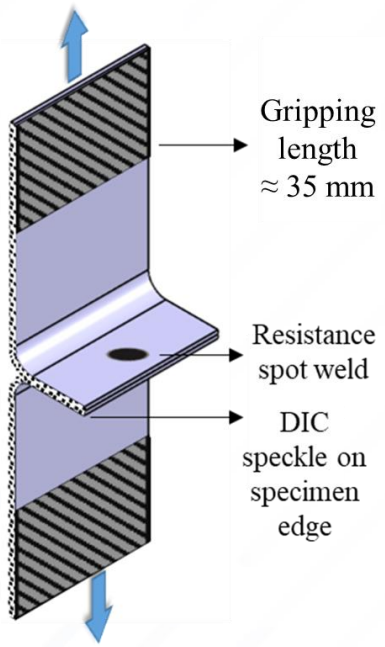

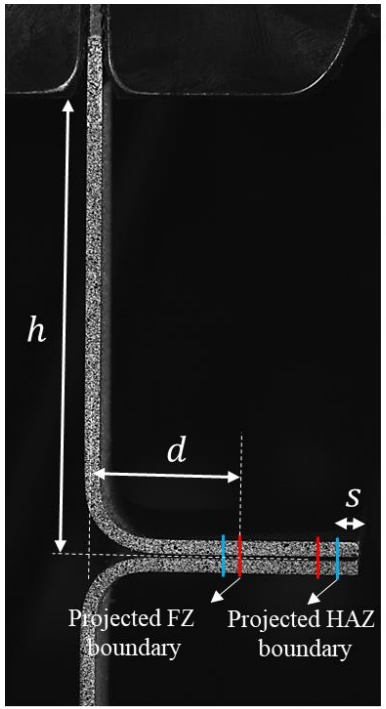

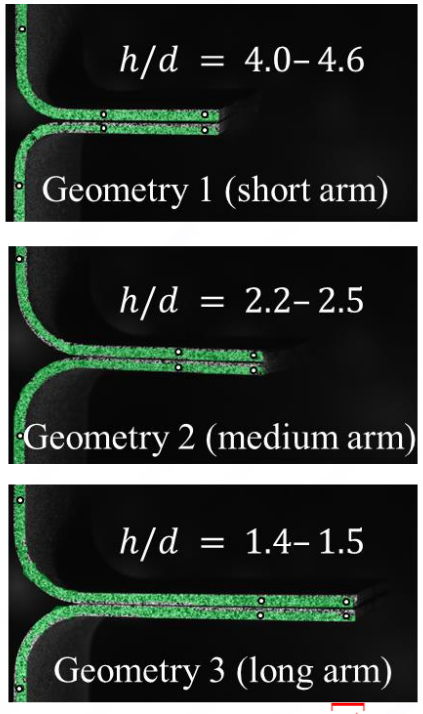

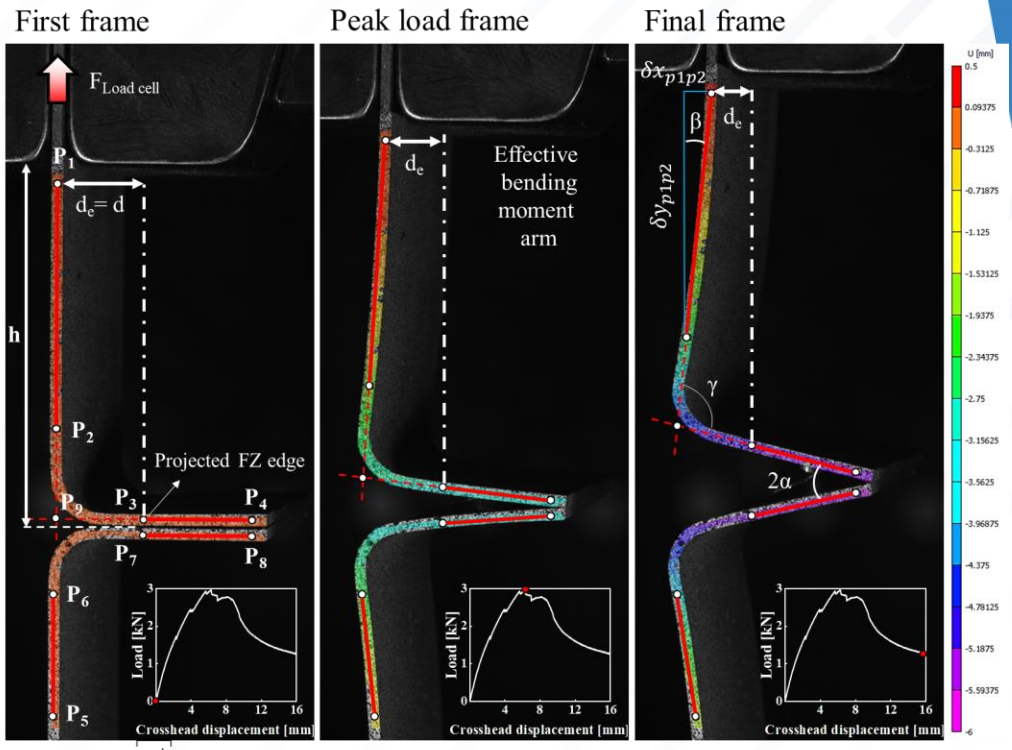

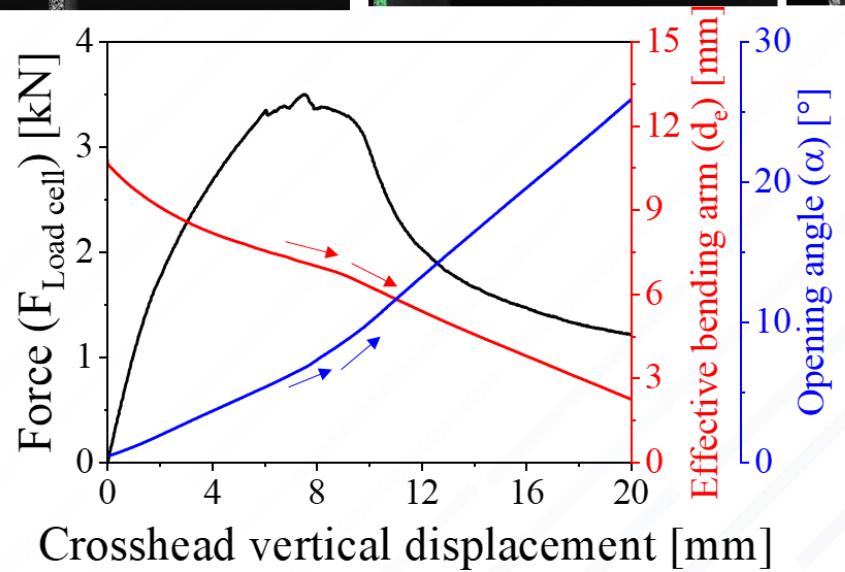

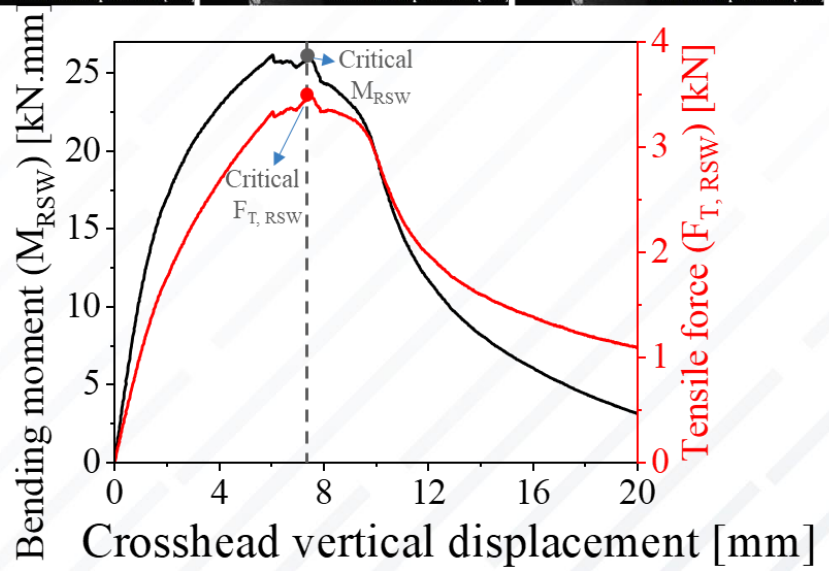

Assessment of Seeger's Loci in Tensile-bending Loading Conditions:

$$f^S = \left[\frac{F_s}{S_S}\right]^a + \left[\frac{F_n}{S_N}\right]^b + \left[\frac{M_b}{S_B}\right]^c \leq 1$$

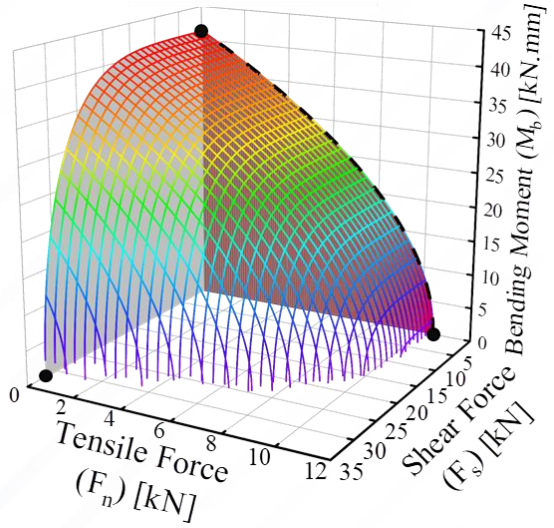

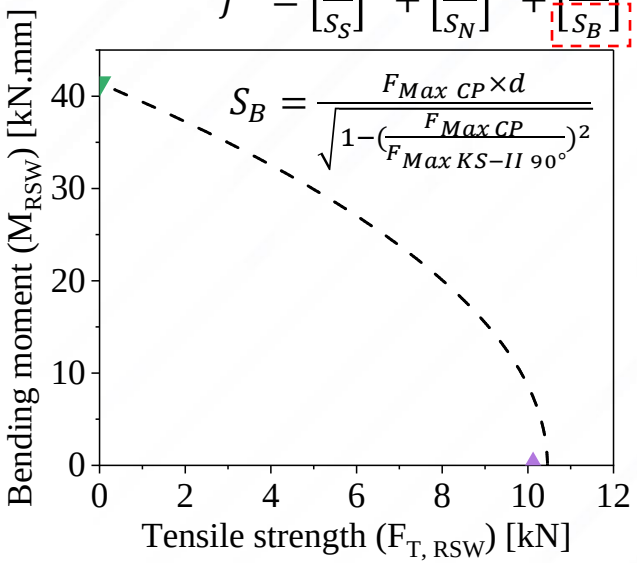

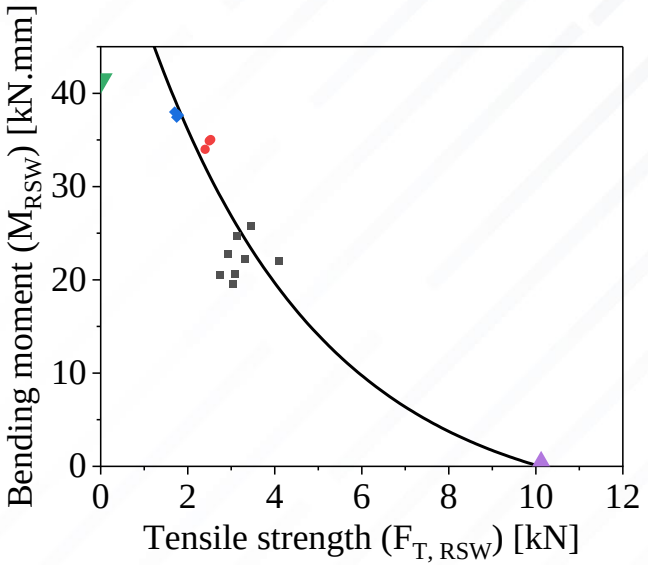

3G-980

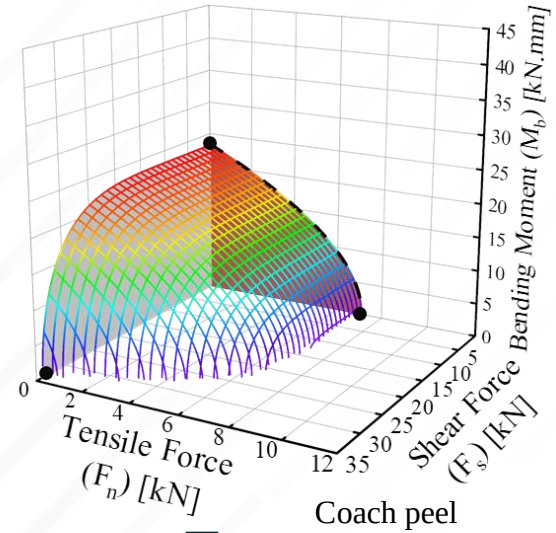

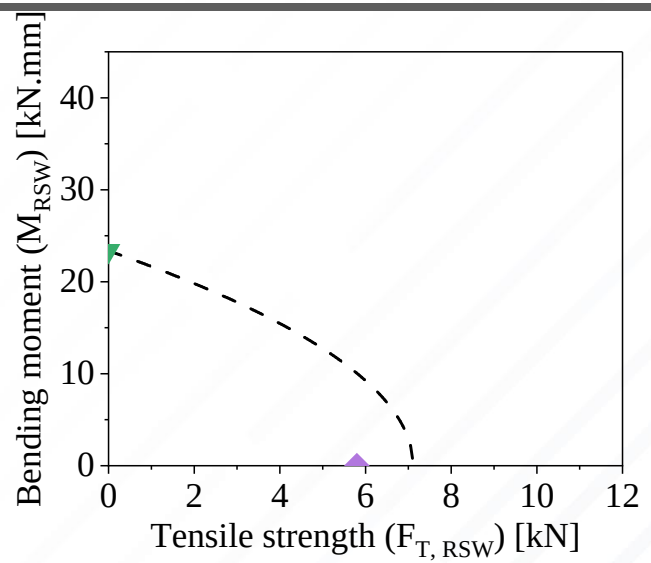

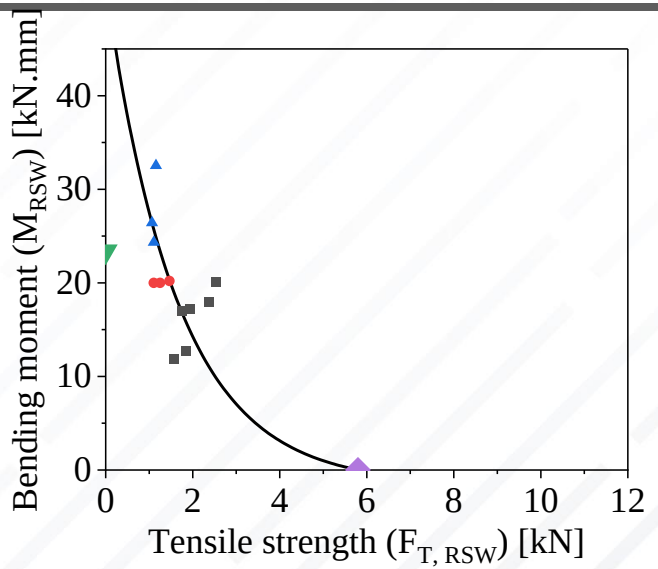

3G-1180

Coach peel (short arm)

Coach peel (medium arm)

Coach peel (long arm)

Tensile strength (KS-II 90°)

Bending strength (S_B)

Summary

GDIS

Part 1

- Four in-situ post-weld heat treatment schedules namely tempering, recrystallization, slow cooling and dual force were compared in the study and all techniques resulted in improved joint performance.

- The optimal post-weld heat treatment schedule was the in-situ grain refinement which resulted in 89% improvement in energy absorption capability compared to the baseline condition and was achieved at a shorter time compared to tempering.

Part 2

- Accuracy of conventional load-based RSW failure loci was assessed in two loading conditions: Shear-tensile combined loading and tensile-bending loading conditions.
- Existing RSW failure loci were accurate in shear-tensile loading condition with over-predictions of between 0.2% to 3.5%.
- Existing failure loci were not accurate in tensile-bending loading conditions. The assumption of a convex failure loci in tensile-bending loading condition results in over-prediction of RSW failure strength by 66%.
- Suitable alternative failure loci were calibrated for the investigated 3G-AHSS that can be directly implemented in load-based failure models.

Acknowledgement

Supervisors:

Tingting Zhang[2], Hassan Ghassemi-Armaki[3], Michael Worswick[1], Cliff Butcher[1], Elliot Biro[1]

[1] Department of Mechanical and Mechatronics Engineering, University of Waterloo, 200 University Avenue West, Waterloo, Ontario, N2L 3G1, Canada

[2] General Motors, Advanced Materials Technology and Virtualization, Warren, MI, USA

[3] General Motors R&D, Manufacturing Systems Research Laboratory, Michigan, USA

For More Information

Olakunle Betiku

PhD Candidate

University of Waterloo, Canada

olakunle.betiku@uwaterloo.ca

Mohammad Shojaee

PhD Candidate

University of Waterloo, Canada

mshojaee@uwaterloo.ca